JB Journals.ASM.org

Biosynthesis of Cell Envelope-Associated Phenolic Glycolipids in *Mycobacterium marinum*

Olivia Vergnolle,[a*] Sivagami Sundaram Chavadi,[a*] Uthamaphani R. Edupuganti,[a] Poornima Mohandas,[a,b] Catherine Chan,[a] Julie Zeng,[a] Mykhailo Kopylov,[a*] Nicholas G. Angelo,[c] J. David Warren,[c] Clifford E. Soll,[d] Luis E. N. Quadri[a,b]

Department of Biology, Brooklyn College, City University of New York, Brooklyn, New York, USA[a]; Graduate Center, City University of New York, New York, New York, USA[b]; Department of Biochemistry and Milstein Chemistry Core Facility, Weill Cornell Medical College, New York, New York, USA[c]; Department of Chemistry, Hunter College, City University of New York, New York, New York, USA[d]

Phenolic glycolipids (PGLs) are polyketide synthase-derived glycolipids unique to pathogenic mycobacteria. PGLs are found in several clinically relevant species, including various *Mycobacterium tuberculosis* strains, *Mycobacterium leprae*, and several nontuberculous mycobacterial pathogens, such as *M. marinum*. Multiple lines of investigation implicate PGLs in virulence, thus underscoring the relevance of a deep understanding of PGL biosynthesis. We report mutational and biochemical studies that interrogate the mechanism by which PGL biosynthetic intermediates (*p*-hydroxyphenylalkanoates) synthesized by the iterative polyketide synthase Pks15/1 are transferred to the noniterative polyketide synthase PpsA for acyl chain extension in *M. marinum*. Our findings support a model in which the transfer of the intermediates is dependent on a *p*-hydroxyphenylalkanoyl-AMP ligase (FadD29) acting as an intermediary between the iterative and the noniterative synthase systems. Our results also establish the *p*-hydroxyphenylalkanoate extension ability of PpsA, the first-acting enzyme of a multisubunit noniterative polyketide synthase system. Notably, this noniterative system is also loaded with fatty acids by a specific fatty acyl-AMP ligase (FadD26) for biosynthesis of phthiocerol dimycocerosates (PDIMs), which are nonglycosylated lipids structurally related to PGLs. To our knowledge, the partially overlapping PGL and PDIM biosynthetic pathways provide the first example of two distinct, pathway-dedicated acyl-AMP ligases loading the same type I polyketide synthase system with two alternate starter units to produce two structurally different families of metabolites. The studies reported here advance our understanding of the biosynthesis of an important group of mycobacterial glycolipids.

Mycobacterial infections are responsible for devastating morbidity and mortality worldwide (1–5). A critical player in the ability of the mycobacteria to produce disease is a formidable cell envelope believed to be responsible for the intrinsic resilience of the mycobacteria to inhospitable environments, antimicrobial agents, and host immune defenses (6–12). Among the unique components found in the cell envelope of several pathogenic mycobacteria are two structurally related families of glycosylated and nonglycosylated lipids commonly referred to as phenolic glycolipids (PGLs) and phthiocerol dimycocerosates (PDIMs), respectively (for a review, see reference 13). PGLs and PDIMs have unusual lipid scaffolds consisting of β-diol-containing, long-chain, aliphatic polyketides esterified with long-chain, multimethyl-branched fatty acids onto the diol functionality (Fig. 1). PGLs and PDIMs are found in several mycobacterial pathogens (e.g., *Mycobacterium tuberculosis* strains, *Mycobacterium bovis*, *Mycobacterium leprae*, and *Mycobacterium marinum*) and thought to be constituents of the characteristic mycobacterial outer membrane. Multiple lines of investigation have provided considerable support for the idea that PGLs and PDIMs are implicated in virulence via complex mechanisms of action that are not fully elucidated (14–32). These (glyco)lipids are also believed to strengthen the cell envelope permeability barrier (20, 33) and to increase the bacterium's intrinsic resistance to antimicrobial drugs (20, 22, 34).

The relevance of PGLs in mycobacterial biology underscores the importance of developing a comprehensive knowledge of the PGL biosynthetic pathway, which remains incompletely understood. Our previous studies of the PGL biosynthetic pathway have revealed a functional cooperation between the *M. marinum* proteins FadD22 (*p*-hydroxybenzoate-AMP ligase/initiation module) and Pks15/1 (iterative type I polyketide synthase [PKS]) for production of *p*-hydroxyphenylalkanoate (PHPA) intermediates required for PGL biosynthesis (35, 36). The PHPA intermediates synthesized by the *M. marinum* FadD22-Pks15/1 iterative system, which is conserved in PGL producers, are thought to be further extended to form the phenolphthiocerol moiety of PGLs (Fig. 1). The extension of the PHPA intermediates has been proposed to be carried out by the modular type I PKS system PpsABCDE, a noniterative synthase complex known to extend fatty acids to form

Received 5 December 2014 **Accepted** 30 December 2014

Accepted manuscript posted online 5 January 2015

Citation Vergnolle O, Chavadi SS, Edupuganti UR, Mohandas P, Chan C, Zeng J, Kopylov M, Angelo NG, Warren JD, Soll CE, Quadri LEN. 2015. Biosynthesis of cell envelope-associated phenolic glycolipids in *Mycobacterium marinum*. J Bacteriol 197:1040–1050. doi:10.1128/JB.02546-14.

Editor: G. A. O'Toole

Address correspondence to Luis E. N. Quadri, LQuadri@brooklyn.cuny.edu.

* Present address: Olivia Vergnolle and Sivagami Sundaram Chavadi, Albert Einstein College of Medicine, Bronx, New York, USA; Mykhailo Kopylov, Florida State University, Tallahassee, Florida, USA.

O.V. and S.S.C. contributed equally to this work.

This paper is dedicated to the memory of our wonderful colleague Clifford E. Soll, who recently passed away.

Supplemental material for this article may be found at http://dx.doi.org/10.1128/JB.02546-14.

doi:10.1128/JB.02546-14

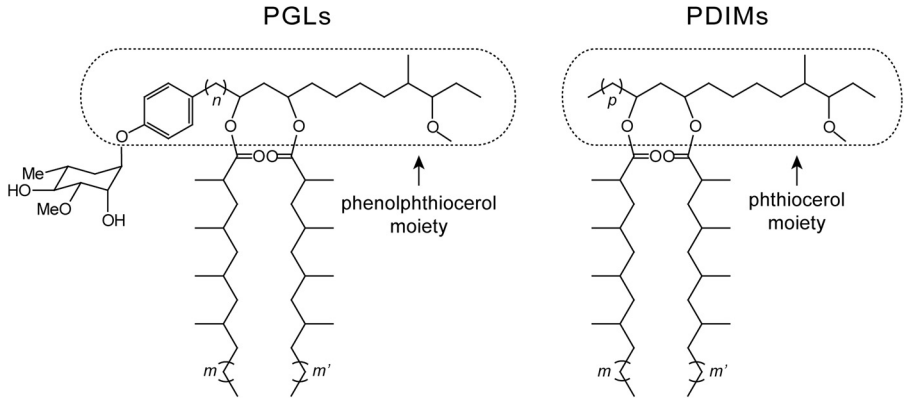

FIG 1 Representative structures of mycobacterial PGLs and PDIMs. The carbon chain variability and glycosyl unit represented are from main variants found in the opportunistic human pathogen *M. marinum*. *m* and *m*', 16 to 20; *n*, 16 to 22; *p*, 14 to 22.

the phthiocerol moiety of PDIMs in *M. tuberculosis* and conserved in PGL/PDIM producers (13, 16, 25, 37, 38) (Fig. 1). However, the mechanism by which the PHPA intermediates assembled by the FadD22-Pks15/1 system would be transferred to the PpsABCDE system for acyl chain extension remains to be experimentally investigated, and the ability of the PpsABCDE system to extend PHPA intermediates has yet to be validated.

Here, we report mutational and biochemical studies that interrogate the mechanism by which the PHPA intermediates are transferred to PpsA, the first-acting enzyme of the PpsABCDE system, and probe the ability of PpsA to extend these intermediates. The studies were conducted with *M. marinum*, a nontuberculous mycobacterial species that is the closest genetic relative of the *M. tuberculosis* complex, is often utilized to model aspects of *M. tuberculosis* biology, and offers greater experimental tractability than other PGL/PDIM producers (39–42). The findings of our studies support a mechanistic model in which the PHPA intermediates are activated and loaded onto the loading acyl carrier protein (ACP_L) domain of *M. marinum* PpsA by a dedicated PHPA-AMP ligase. Our results also demonstrate that *M. marinum* PpsA is capable of extending PHPA intermediates. The conservation of the PGL biosynthetic genes across species (13, 43) (Fig. 2) and studies of members of the *M. tuberculosis* complex (44) strongly suggest that the mechanistic insights into PGL biosynthesis gained here are applicable to other PGL producers. Overall, these studies advance our understanding of the biosynthesis of an important group of mycobacterial cell envelope-associated glycolipids.

MATERIALS AND METHODS

Culturing conditions, recombinant DNA manipulations, and reagents. *M. marinum* strain M (ATCC BAA-535) and its derivatives were cultured under standard conditions in Middlebrook 7H9 medium (Difco) supplemented with 10% ADN (5% bovine serum albumin [BSA], 2% dextrose, 0.85% NaCl) and 0.05% Tween 80 (supplemented 7H9) or on Middlebrook 7H11 agar (Difco) with ADN (supplemented 7H11) (45). The strains used in this study are listed in Table S1 in the supplemental material. *Escherichia coli* strains were cultured under standard conditions in Luria-Bertani (LB) medium (46). When required, kanamycin (30 μg ml^{-1}), hygromycin (50 μg ml^{-1}), sucrose (2%), and/or 5-bromo-4-chloro-3-indolyl-β-D-galactopyranoside (X-Gal; 70 μg ml^{-1}) were added to the growth media. DNA manipulations were carried out by standard methods and using *E. coli* DH5α (Invitrogen) as the primary cloning host (46). All PCR-generated DNA fragments used in plasmid constructions were sequenced to verify fidelity. The plasmids used in this study are listed in Table S2 in the supplemental material. Genomic DNA isolation and plasmid electroporation into mycobacteria were carried out as reported previously (45). Molecular biology reagents were obtained from Sigma, Invitrogen, Novagen, or Qiagen. The oligonucleotides used in this study are listed in Tables S3 and S4 in the supplemental material, and they were purchased from Integrated DNA Technologies, Inc. Solvents and nonradiolabeled chemicals were purchased from Sigma, Acros Organics, or Fisher Scientific. [1-^{14}C]propionate (specific activity, 54 mCi $mmol^{-1}$)

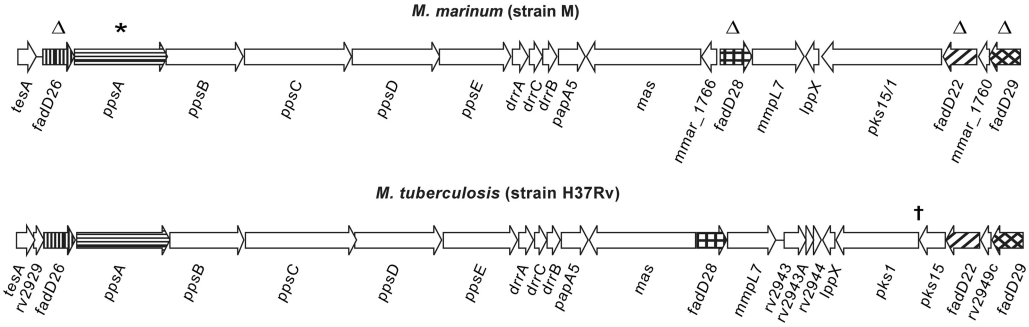

FIG 2 Conservation of *M. marinum* and *M. tuberculosis* chromosomal loci involved in PGL-PDIM production. The five *M. marinum* genes targeted for mutational analysis (Δ, deletion; *, amino acid substitution) in this study and their respective orthologs in *M. tuberculosis* are highlighted with pattern-filled arrows. †, *pks15/1* is essential for PGL production. The gene *pks15/1* is disrupted (split into *pks1* and *pks15*) by natural mutations in *M. tuberculosis* H37Rv and other Euro-American lineage strains, thus leading to PGL deficiency (18, 64). Additional genes implicated in PGL and/or PDIM production located downstream of *fadD29* are not depicted. Adapted from reference 13 with permission of the publisher.

and [carboxyl-^{14}C]*p*-hydroxybenzoic acid (specific activity, 55 mCi mmol^{-1}) were acquired from American Radiolabeled Chemicals, Inc. The compound 21-(4-hydroxyphenyl)henicosanoic acid (s-PHPA) was synthesized as described in the supplemental material.

Construction of mycobacterial mutants. The mutants were engineered using the p2NIL/pGOAL19-based flexible cassette method (47) as reported previously (34, 35, 48). A gene-specific mutagenesis cassette delivery vector (see below) was used to construct each mutant. Each vector was electroporated into *M. marinum*, and the transformants with a potential single crossover (blue colonies) were selected on supplemented 7H11 containing hygromycin, kanamycin, and X-Gal. Potential single-crossover-bearing clones were grown in antibiotic-free supplemented 7H9 and then plated for single colonies on supplemented 7H11 containing sucrose and X-Gal. White colonies that grew on sucrose plates were restreaked onto antibiotic-free and antibiotic-containing plates to identify drug-sensitive clones, a trait indicating a possible double-crossover event with consequent allelic replacement or reversion to wild type (wt). Gene deletions were confirmed by PCR. For PCR analysis, genomic DNA from mutant candidates was used as the template along with two independent mutant-specific primer pairs (see Table S3 in the supplemental material) to produce amplicons permitting differentiation between mutant and wt genotypes based on amplicon size (see Fig. S2 in the supplemental material). Nucleotide substitutions in the *M. marinum ppsA*$_{\text{S-to-A}}$ mutant were confirmed by DNA sequencing. The mutated region was PCR amplified with specific primers (see Table S3 in the supplemental material), and the resulting amplicon was sequenced (see Fig. S2 in the supplemental material).

Construction of mutagenesis cassette delivery vectors. The following mutagenesis cassette delivery vectors were constructed: p2NILGOALc-Δ*fadD22*c, carrying a *fadD22* (MMAR_1761) deletion cassette (Δ*fadD22*c); p2NILGOALc-Δ*fadD26*c, carrying a *fadD26* (MMAR_1777) deletion cassette (Δ*fadD26*c); p2NILGOALc-Δ*fadD28*c, carrying a *fadD28* (MMAR_1765) deletion cassette (Δ*fadD28*c); p2NILGOALc-Δ*fadD29*c, carrying a *fadD29* (MMAR_1759) deletion cassette (Δ*fadD29*c); and p2NILGOALc-*ppsA*c, carrying a *ppsA* (MMAR_1776) mutagenesis cassette (*ppsA*c) (see Fig. S1 and Table S2 in the supplemental material). Each cassette was constructed by joining a 5′ arm and a 3′ arm using splicing by overlap extension (SOE) PCR (49). The primers and amplicon sizes are shown in Table S4 in the supplemental material. Each PCR-generated cassette was first cloned into pCR2.1-TOPO (Invitrogen), verified for sequence fidelity, and then subcloned into p2NIL (47). The cassettes Δ*fadD22*c, Δ*fadD26*c, Δ*fadD28*c, Δ*fadD29*c, and *ppsA*c were cloned into p2NIL as SalI-NotI, HindIII-KpnI, BamHI-NotI, HindIII-PmlI, and HindIII-HpaII fragments, respectively. Each resulting p2NIL-mutagenesis cassette construct and the plasmid pGOAL19 (47) were digested with PacI, and then the PacI fragment with the marker cassette (GOALc) of pGOAL19 was ligated to the p2NIL construct backbones to generate the final delivery vectors. The configuration of each final cassette was as follows: Δ*fadD22*c consisted of *fadD22*'s 1,000-bp upstream segment plus *fadD22*'s first 2 codons plus *fadD22*'s last 2 coding codons plus stop codon plus 983-bp downstream segment; Δ*fadD26*c consisted of *fadD26*'s 962-bp upstream segment plus *fadD26*'s first 5 codons plus *fadD26*'s last 3 coding codons plus stop codon plus 929-bp downstream segment; Δ*fadD28*c consisted of *fadD28*'s 947-bp upstream segment plus *fadD28*'s first 5 codons plus *fadD28*'s last 4 coding codons plus stop codon plus 935-bp downstream segment; Δ*fadD29*c consisted of *fadD29*'s 947-bp upstream segment plus *fadD29*'s first 4 codons plus *fadD29*'s last 5 coding codons plus stop codon plus 976-bp downstream segment; and *ppsA*c consisted of a 1,832-bp segment with Ser-to-Ala substitution mutations in the center.

Construction of pCP0 derivatives. Plasmids pCP0-*fadD22*, pCP0-*fadD26*, pCP0-*fadD28*, pCP0-*fadD29*, and pCP0-*ppsA*, constitutively expressing *fadD22*, *fadD26*, *fadD28*, *fadD29*, and *ppsA*, respectively, from the mycobacterial *hsp60* promoter were constructed using the expression vector pCP0 (34). DNA fragments each encompassing an *M. marinum* gene and its predicted ribosome-binding site were PCR generated using the primer pairs shown in Table S4 in the supplemental material. The fragments were first cloned into pCR2.1-TOPO, verified for sequence fidelity, and then subcloned into pCP0. The *fadD22*, *fadD26*, *fadD28*, *fadD29*, and *ppsA* fragments were cloned into pCP0 as HindIII-HpaI, EcoRI-HindIII, NheI-HindIII, EcoRI-HindIII, and HpaI-NheI inserts, respectively.

Analysis of PGLs and PDIMs. Four-day-old cultures were diluted to an optical density at 595 nm (OD_{595}) of 0.6 in supplemented 7H9 and loaded into 12-well plates (1 ml per well). [^{14}C]propionate (which labels both PDIMs and PGLs) or [^{14}C]*p*-hydroxybenzoic acid (which selectively labels PGLs) was added to each well (0.2 μCi ml^{-1}), and the plates were incubated for 24 h (30°C, 170 rpm). After incubation, the OD_{595} of the cultures was measured in a plate reader (Beckman Coulter, Inc.) and the cells were harvested for apolar lipid fraction extraction with a biphasic mixture of methanolic saline and petroleum ether as reported previously (35, 50). Lipid extracts were subjected to radiometric thin-layer chromatography (radio-TLC) for analysis of ^{14}C-labeled PGLs and ^{14}C-labeled PDIMs as described earlier (35, 50). Developed TLC plates were exposed to phosphor screens, which were scanned using a Cyclone Plus Storage Phosphor System (PerkinElmer, Inc.).

Construction of pETDuet-PpsA. *M. marinum ppsA* was assembled from three fragments: NT1 (5′-end fragment, 2,100 bp); NT2 (middle fragment, 2,000 bp); and NT3 (3′-end fragment, 809 bp). The fragments were PCR amplified from genomic DNA with fragment-specific primers (see Table S4 in the supplemental material) and independently cloned into pCR2.1-TOPO to create pCR2.1TOPO-PpsA-NT1, pCR2.1TOPO-PpsA-NT2, and pCR2.1TOPO-PpsA-NT3. The inserts were verified for sequence fidelity. Subsequently, the NT1 insert of pCR2.1TOPO-PpsA-NT1 was recovered as a BamHI-AscI fragment and subcloned into pETDuet-1 (Novagen) digested with the same enzymes to create pETDuet-PpsA-NT1. Then, the NT2 insert of pCR2.1TOPO-PpsA-NT2 was recovered as an SpeI-AscI fragment and subcloned into SpeI-AscI linearized pETDuet-PpsA-NT1, resulting in pETDuet-PpsA-NT1NT2. Finally, the NT3 insert of pCR2.1TOPO-PpsA-NT3 was recovered as an AscI-HindIII fragment and subcloned into pETDuet-PpsA-NT1NT2 digested with the same enzymes to generate pETDuet-PpsA. This final plasmid was introduced into *E. coli* BAP1 (51) for isopropyl β-D-1-thiogalactopyranoside (IPTG)-inducible production of N-terminally His_6-tagged PpsA.

Construction of pCOLADuet-FadD29. *M. marinum fadD29* was PCR amplified from genomic DNA with gene-specific primers (see Table S4 in the supplemental material) and cloned into pCR2.1-TOPO to create pCR2.1TOPO-FadD29. The insert of pCR2.1TOPO-FadD29 was verified for sequence fidelity, recovered as an EcoRI-NotI fragment, and subcloned into pCOLADuet-1 (Novagen) linearized with EcoRI and NotI to generate pCOLADuet-FadD29. This final plasmid was introduced into *E. coli* BL21(DE3) (Stratagene) for IPTG-inducible production of N-terminally His_6-tagged FadD29.

Overproduction and purification of PpsA. *E. coli* BAP1 carrying pETDuet-PpsA was cultured in LB broth supplemented with ampicillin (100 μg ml^{-1}) at 37°C with orbital shaking (220 rpm) to an OD_{600} of 0.6. When the culture reached the target OD, the incubation temperature was reduced to 18°C, and PpsA expression was induced with IPTG (0.1 mM). After 20 h of additional incubation (18°C, 220 rpm), cells were harvested by centrifugation (6,000 × *g*, 20 min). The cell pellet was resuspended in lysis buffer (75 mM sodium phosphate [pH 7.5], 500 mM NaCl, 10% glycerol, 10 mM imidazole), and cells were disrupted using a high-pressure homogenizer (Avestin, Inc.). Cellular debris was removed from the lysate by centrifugation (1 h, 12,000 rpm, FX6100 rotor; Beckman Coulter Inc.) followed by subsequent filtration of the supernatant (0.45-μm filter). PpsA was purified from the clarified supernatant by Ni^{2+} column chromatography using Ni-nitrilotriacetic acid (Ni-NTA) Superflow resin according to the manufacturer's instructions (Qiagen). Proteins were eluted from the column using an imidazole gradient in lysis buffer run

with an ÄKTA UPC10 fast protein liquid chromatography (FPLC) system (GE Healthcare). PpsA eluted at 125 mM imidazole. Fractions with the best purity were identified by sodium dodecyl sulfate polyacrylamide gel electrophoresis (SDS-PAGE), pooled, concentrated using Amicon Ultra-15 centrifugal filter devices (50-kDa cutoff), and buffer exchanged into 100 mM sodium phosphate buffer (pH 7.2) using PD-10 desalting columns (GE Healthcare). Protein samples were aliquoted with 25% glycerol final concentration, flash-frozen in liquid nitrogen, and stored at −80°C (see Fig. S3 in the supplemental material). A typical yield was 14 mg liter^{-1}.

Overproduction and purification of FadD29. *E. coli* BL21(DE3) carrying pCOLADuet-FadD29 was cultured in LB broth containing kanamycin at 37°C with orbital shaking (220 rpm). When the culture reached an $OD_{600\ nm}$ of 0.6, the incubation temperature was reduced to 30°C, and FadD29 production was induced with IPTG (0.1 mM). After 20 h of additional incubation (30°C, 220 rpm), cells were harvested by centrifugation and resuspended in lysis buffer (50 mM Tris-HCl, 500 mM NaCl [pH 7.5], 10 mM imidazole). Cell disruption and removal of cellular debris from the lysate were carried out as noted above. FadD29 was purified from the clarified supernatant by Ni^{2+} column chromatography. Proteins were eluted from the column using an imidazole gradient in lysis buffer run with an ÄKTA UPC10 FPLC system. FadD29 eluted at 140 mM imidazole. Fractions with the best purity were identified by SDS-PAGE, pooled, concentrated using Amicon Ultra-15 centrifugal filter devices (30-kDa cutoff), and buffer exchanged into 50 mM Tris-HCl–300 mM NaCl (pH 7.8) using PD-10 desalting columns. Purified proteins were aliquoted with 25% glycerol (final concentration), flash-frozen in liquid nitrogen, and stored at −80°C (see Fig. S3 in the supplemental material). A typical yield was 6.3 mg liter^{-1}.

***In vitro* FadD29-PpsA reconstituted system.** The standard complete reaction mixture (250 μl) contained 0.5 μM FadD29, 5.0 μM PpsA, 2.5 μM s-PHPA, 100 mM sodium phosphate buffer (pH 7.2), 1 mM tris(2-carboxyethyl)phosphine (TCEP), 0.5 mM $MgCl_2$, 0.5 mM ATP, 10% glycerol, 0.1 mM malonyl coenzyme A (malonyl-CoA) thioester, and 1 mM NADPH. After incubation (30°C, 2.5 h), the reaction was quenched by the addition of 50 μl of 1 M NaOH, and then the mixture was incubated at 65°C for 20 min to release the covalently bound products from PpsA. Following the alkaline hydrolysis, the reaction mixture was acidified with 50 μl of 2 M HCl, and the reaction products were extracted with ethyl acetate (750 μl × 2). The recovered organic layer was evaporated to dryness. The dried residual material was dissolved in 50 μl of dichloromethane and analyzed by high-resolution liquid chromatography-mass spectrometry (LC-MS) as described below. Control reaction mixtures lacking selected components were also set up, treated, and analyzed in the same manner as the complete reaction mixture.

Liquid chromatography-mass spectrometry instrumentation and analysis. Mass spectral data were collected on an Agilent Technologies G6550A iFunnel high-resolution quadrupole time of flight (Q-TOF) mass spectrometer attached to an Agilent Technologies 1290 ultrahigh-performance liquid chromatography (UHPLC) system. Samples were ionized using Agilent's dual-sprayer Jet Stream electrospray ionization source (Dual AJS ESI) with the analysis performed in negative mode. Chromatography was performed on an Agilent Technologies Poroshell 120 EC-C_8 column (2.1 mm by 75 mm, 2.7 μm) using water containing 0.1% formic acid (solvent A) and methanol containing 0.1% formic acid (solvent B) at a flow rate of 350 μl min^{-1}. The UHPLC gradient was 75% solvent B (0 min) to 100% solvent B (15 min), and the analysis was stopped after 20 min. The column was equilibrated under the starting conditions for 10 min and held at 45°C for the entire analysis. The UHPLC stream was diverted to waste for the first 1.5 min of the analysis. Mass spectrometer parameters for the MS were as follows: 225°C drying gas temperature; 17-liters min^{-1} drying gas flow; 35-lb/in^2 nebulizer pressure; 200°C sheath gas temperature; 12-liters min^{-1} sheath gas flow; 3,500-V capillary voltage; 2,000-V nozzle voltage; and 365-V fragmentor. Data were collected with the instrument set to low mass range (100 to 1,700 *m*/*z*) and extended dynamic range conditions (2 GHz mode) at 2 spectra per second. Both centroid and profile data were stored (1.5 to 20 min) with a threshold of 300 counts for MS mode. The reference masses 112.985587 *m*/*z* (trifluoroacetate ion) and 966.000725 *m*/*z* (HP 921 reference compound + formate ion) were infused into the spray chamber through the second sprayer using an Agilent binary pump. A minimum height of 5,000 counts and a 100 ppm window were used. The instrument was controlled with Agilent MassHunter Workstation Acquisition Software B.05.00. The data were analyzed using Agilent MassHunter Workstation Qualitative Analysis Software B.05.00.

RESULTS AND DISCUSSION

Possible pathways for Pks15/1-to-PpsA PHPA intermediate transfer in *M. marinum*. Previous studies have shown that the conserved modular (noniterative) type I PKS system PpsABCDE encoded in the PGL/PDIM biosynthetic gene cluster of *M. tuberculosis* (Fig. 2) extends fatty acids to form the phthiocerol moiety of PDIMs (Fig. 1). The fatty acids are activated and loaded by the conserved fatty acyl-AMP ligase FadD26 (Fig. 2) onto the loading acyl carrier protein (ACP_L) domain of PpsA, the first-acting enzyme of the PpsABCDE system (37, 52). The PpsABCDE system is proposed to also extend pathway-dedicated PHPA intermediates synthesized by the conserved iterative PKS system FadD22-Pks15/1 (Fig. 2) to form the phenolphthiocerol moiety of PGLs (36, 38) (Fig. 1). The mechanism by which PHPA intermediates synthesized by the iterative FadD22-Pks15/1 system would be transferred to the noniterative PpsABCDE system for chain extension has not been experimentally interrogated.

We hypothesized two possible pathways by which this PHPA intermediate transfer could take place in *M. marinum* (Fig. 3). In one of these pathways (Fig. 3, pathway A), the intermediates would be released first from the phosphopantetheinyl (P-pant) group of the acyl carrier protein (ACP) domain of Pks15/1 (step A1) and subsequently activated (step A2) and loaded (step A3) by a dedicated PHPA-AMP ligase onto the P-pant group of the ACP_L domain of PpsA. The PHPA intermediates bound to the ACP_L would be subsequently captured by the ketosynthase (KS) domain (step A4) to generate the loaded PpsA (Fig. 3, boxed acyl-PpsA species) ready for KS domain-dependent decarboxylation/condensation. The Pks15/1-to-PpsA PHPA intermediate transfer mechanism represented in pathway A (Fig. 3) emerges from analogy to the fatty acyl-AMP ligase-dependent mechanism of fatty acid activation and loading onto the ACP_L domain of PpsA during PDIM biosynthesis in *M. tuberculosis* (52). Pathway A is further supported by recent studies in the *M. tuberculosis* complex, leading to the proposal that the conserved fatty acyl-AMP ligase FadD29 (Fig. 2) loads PHPAs onto PpsA (44), yet this idea remains to be experimentally validated.

Notably, pathway A (Fig. 3) requires free PHPA intermediates (step A1), yet sequence analysis of Pks15/1 orthologs does not reveal the presence of a possible thioesterase domain that would conveniently catalyze the release of the PHPA intermediates thioesterified to the P-pant group of the ACP domain of the synthase (13, 36). This does not rule out, however, the possibility that the PHPA intermediates are released without the assistance of an external (self-standing) thioesterase or by the action of one. In the latter option, the thioesterase could be TesA, which is encoded in the PGL/PDIM biosynthetic gene cluster (Fig. 2) and was recently shown to be required for PGL and PDIM production in *M. marinum* (22, 34).

In the second possible pathway for Pks15/1-to-PpsA PHPA

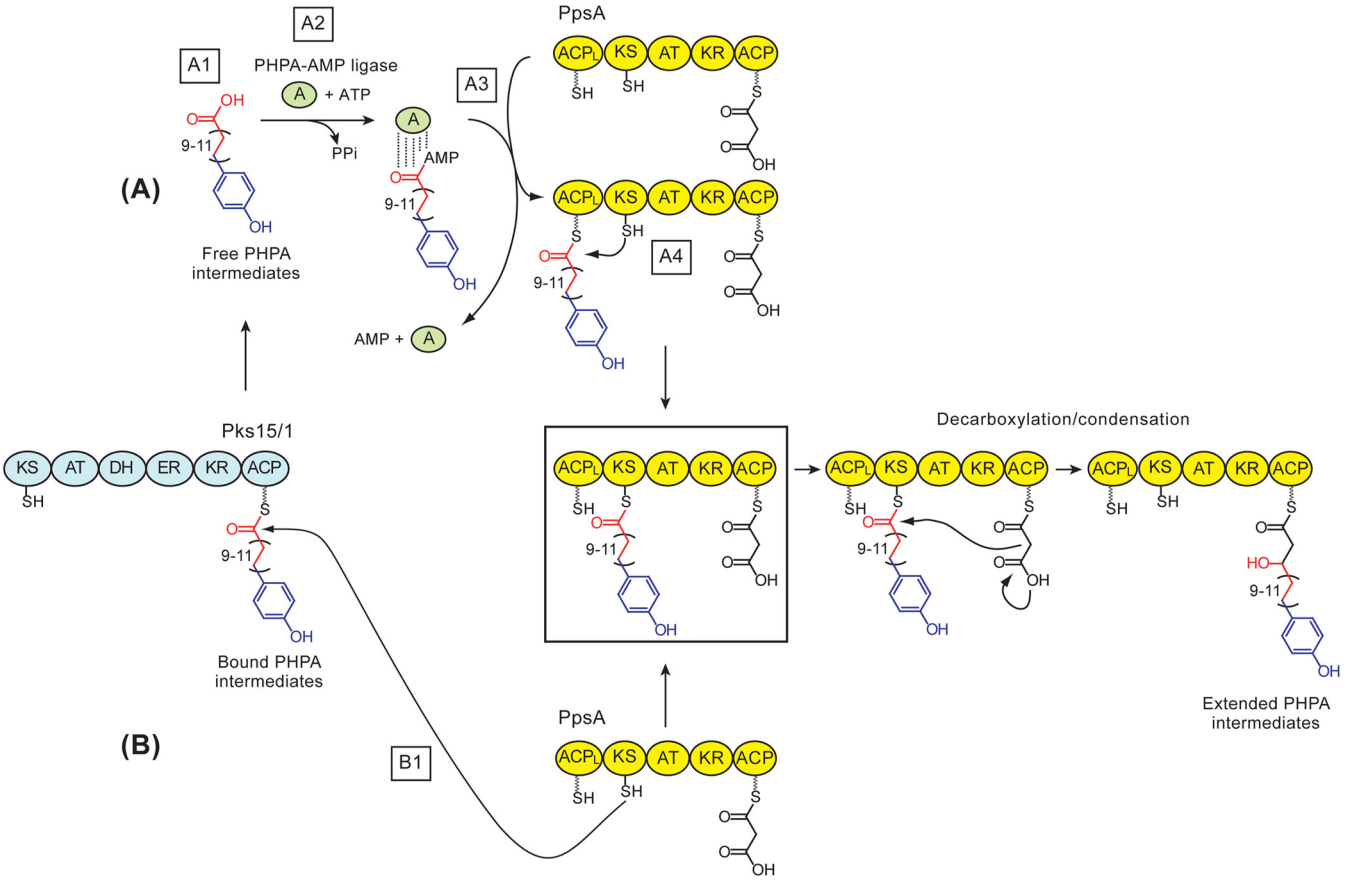

FIG 3 Two possible mechanisms for transfer of *p*-hydroxyphenylalkanoate (PHPA) intermediates to PpsA in *M. marinum*. (A) PHPA-AMP ligase-dependent model. The model includes the release of PHPAs thioesterified to Pks15/1's ACP domain (A1), activation of free PHPAs by a PHPA-AMP ligase (A2), PHPA-AMP ligase-dependent loading of PHPAs onto PpsA's ACP_L domain (A3), and capture of the ACP_L domain-bound PHPAs by PpsA's KS domain to yield the fully loaded PpsA (boxed) ready for KS domain-dependent decarboxylation/condensation. (B) Direct KS domain capture model. In this model, the fully loaded PpsA (boxed) is generated directly by the capture of Pks15/1-bound PHPAs by PpsA's KS domain (B1), thus bypassing the need for steps A1 through A4. Decarboxylation/condensation leads to extension of PHPAs by a 2-carbon unit via the first noniterative extension cycle in the formation of phenolphthiocerols. In the scheme, the depicted carbon chain variability in the PHPA-Pks15/1 thioester intermediate is that expected during synthesis of *M. marinum* PGLs. Adenylated PHPAs are shown bound to the PHPA-AMP ligase via noncovalent linkages (by analogy to other acyl adenylating enzymes). PpsA's C-terminal ACP domain is shown loaded (AT domain dependent) with the malonyl-CoA-derived extender unit. Thiol groups of the phosphopantetheinyl group in the ACP domains and the catalytic Cys in the KS domain are depicted. The hydroxyl group in the extended PHPAs generated from the keto group by action of the KR domain of PpsA is shown. Sections of the PHPA intermediates are color coded based on origin: blue, derived from a *p*-hydroxybenzoic acid starter unit; red, derived from malonyl extender units via iterative extension cycles; black, section derived from a malonyl extender unit via a noniterative extension cycle. Domain abbreviations: A, adenylation; ACP, acyl carrier protein; ACP_L, loading acyl carrier protein; AT, acyltransferase; DH dehydratase; ER, enoylreductase; KR, ketoreductase; KS, ketosynthase.

intermediate transfer in *M. marinum* (Fig. 3, pathway B), the PHPAs thioesterified to the P-pant group of the ACP domain of Pks15/1 would be directly captured by the KS domain of PpsA (step B1), thus bypassing the need for steps A1 to A4. This direct Pks15/1-to-PpsA chain translocation would "skip" the ACP_L domain of PpsA. Domain skipping has in fact been demonstrated in a few PKS systems (53–55). Moreover, this direct-capture pathway would have adaptive value because it would not require ATP for PHPA intermediate activation, an essential step in pathway A (step A2). This pathway would also obviate the need to off-load the PHPA intermediates from the ACP domain of Pks15/1 (pathway A, step A1).

A functional ACP_L domain in PpsA is required for production of both PGLs and PDIMs in *M. marinum*. The ACP_L domain of PpsA requires phosphopantetheinylation of the Ser residue embedded in the P-pant group attachment site motif (NCBI Conserved Domains Database [CDD] no. pfam00550/smart00823) of the domain to become functional (56–58). Phosphopantetheinylation of the ACP_L domain introduces the P-pant group onto which the fatty acids are loaded with the assistance of the fatty acyl-AMP ligase FadD26 to form the fatty acyl-ACP_L domain thioester intermediate required for PDIM biosynthesis in *M. tuberculosis* (37, 52). Formation of the analogous PHPA-ACP_L domain thioester intermediate would be required for PGL production in *M. marinum* if the Pks15/1-to-PpsA PHPA intermediate transfer takes place by the PHPA-AMP ligase-dependent pathway outlined in Fig. 3 (pathway A). On the other hand, formation of the PHPA-ACP_L domain intermediate would not be needed for PGL production if the intermediate transfer proceeds via direct capture by the KS domain of PpsA as depicted in Fig. 3 (pathway B). With these considerations in mind, we probed the essentiality of the P-pant group attachment site of the ACP_L domain of PpsA for PGL pro-

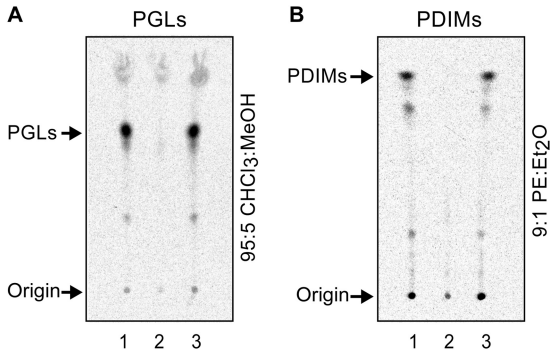

FIG 4 Inactivation of PpsA's ACP_L domain leads to a PGL^- $PDIM^-$ phenotype in *M. marinum*. Radio-TLC analysis of ^{14}C-labeled PGLs (A) and ^{14}C-PDIMs (B) from *M. marinum* wt + pCP0 (lane 1), *M. marinum* $ppsA_{S\text{-}A}$ + pCP0 (lane 2), and *M. marinum* $ppsA_{S\text{-}A}$ + pCP0-*ppsA* (lane 3). The wild-type (wt) and mutant *M. marinum* strains carried the vector pCP0 so they could be cultured in the same kanamycin-containing medium used for the complemented *M. marinum* $ppsA_{S\text{-}A}$ + pCP0-*ppsA* strain. TLC solvent systems used are indicated. $CHCl_3$, chloroform; MeOH, methanol; PE, petroleum ether; Et_2O, diethyl ether.

duction by mutational analysis in *M. marinum*. To this end, we engineered an unmarked, site-directed mutant (*M. marinum* $ppsA_{S\text{-}to\text{-}A}$) with a Ser-to-Ala substitution that eliminated the phosphopantetheinylation site (Ser43) in the ACP_L domain of the synthase. We identified Ser43 as the phosphopantetheinylation target in the P-pant group attachment site sequence motif of the ACP_L domain of PpsA by sequence analysis (not shown). The *M. marinum* $ppsA_{S\text{-}to\text{-}A}$ mutant carried also a Ser42-to-Ala substitution. Ser42 (adjacent to Ser43) was replaced in case it could become a surrogate phosphopantetheinylation target in the absence of Ser43, a potentially confounding scenario.

Evaluation of PGL production in the *M. marinum* $ppsA_{S\text{-}to\text{-}A}$ mutant by radiometric thin-layer chromatography (radio-TLC) analysis revealed that the strain was PGL deficient (Fig. 4A, cf. lanes 1 and 2). Radio-TLC analysis revealed that the mutant strain was also unable to produce PDIMs (Fig. 4B, cf. lanes 1 and 2), a result in line with previous biochemical studies on PDIM biosynthesis in *M. tuberculosis* (37, 52). Introduction of the plasmid pCP0-*ppsA* (expressing *M. marinum ppsA*) into *M. marinum* $ppsA_{S\text{-}to\text{-}A}$ restored the capacity of the mutant to produce both PGLs (Fig. 4A, cf. lanes 2 and 3) and PDIMs (Fig. 4B, cf. lanes 2 and 3). Overall, the findings of the mutational analysis in *M. marinum* are in line with the idea that the Pks15/1-to-PpsA PHPA intermediate transfer takes place by the PHPA-AMP ligase-dependent pathway outlined in pathway A of Fig. 3. The results also suggest that direct capture of the PHPA intermediates thioesterified to the ACP domain of Pks15/1 by the KS domain of PpsA (Fig. 3, pathway B) is not a transfer mechanism of physiological relevance in *M. marinum*.

Mutational analysis in *M. marinum* identifies FadD29 as a PHPA-AMP ligase candidate. The mechanistic model proposed in pathway A (Fig. 3) includes an acyl-AMP ligase competent to activate and load the PHPA intermediates onto the ACP_L domain of *M. marinum* PpsA (steps A2 and A3, respectively). Aside from the *p*-hydroxybenzoic acid-specific adenylation domain of *M. marinum* FadD22 (35, 36), there are three conserved acyl-AMP ligases encoded in the PGL/PDIM biosynthetic gene cluster, i.e., FadD26, FadD28, and FadD29 (13, 16, 25, 37, 43, 52) (Fig. 2). Recent studies in the *M. tuberculosis* complex have led to the proposal that FadD29 adenylates and loads PHPAs onto PpsA in *M. tuberculosis* (44), but the idea has not been experimentally explored.

To seek further support for the mechanistic model proposed in pathway A (Fig. 3), we undertook a systematic mutational analysis to conclusively establish the involvement of *fadD22*, *fadD26*, *fadD28*, and *fadD29* in PGL and PDIM production in *M. marinum* and inform the identification of a PHPA-AMP ligase candidate in a nontuberculous mycobacterial species. To our knowledge, the involvement of *M. marinum fadD22* and *M. marinum fadD29* in the production of PDIMs and PGLs has not been probed by mutational analysis. *M. marinum* mutants with a transposon insertion in the promoter region of *fadD26* or in *fadD28* were recently shown to have defects in PGL and PDIM production, but potentially confounding polar effects produced by the transposon upstream of *fadD26* on other genes of the pathway (*ppsA* to *papA5* genes [Fig. 2]) preclude unequivocal gene-to-function assignment for *fadD26* (20). To conclusively probe the involvement of the four *M. marinum* acyl-AMP ligases encoded in the PGL/PDIM biosynthetic gene cluster in PGL and PDIM production, we engineered four mutants (*M. marinum* Δ*fadD22*, *M. marinum*

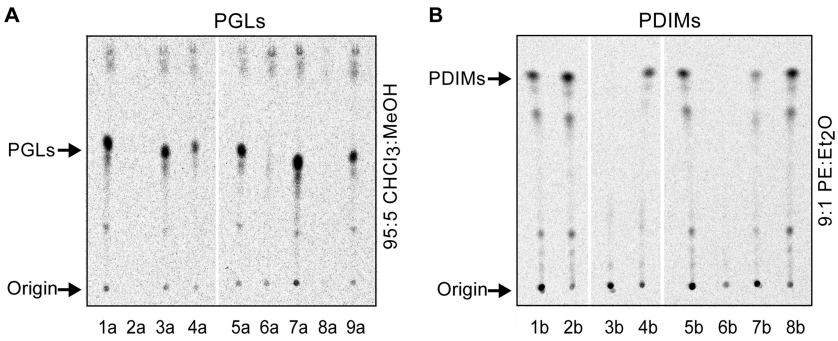

FIG 5 Mutational analysis points at *M. marinum* FadD29 as a PHPA-AMP ligase candidate. Radio-TLC analysis of ^{14}C-labeled PGLs (A) and ^{14}C-PDIMs (B) from *M. marinum* wt + pCP0 (lanes 1a, 5a, 1b, 5b), *M. marinum* Δ*fadD22* + pCP0 (lanes 2a and 2b), *M. marinum* Δ*fadD22* + pCP0-*fadD22* (lane 3a), *M. marinum* Δ*fadD26* + pCP0 (lanes 4a and 3b), *M. marinum* Δ*fadD26* + pCP0-*fadD26* (lane 4b), *M. marinum* Δ*fadD28* + pCP0 (lanes 6a and 6b), *M. marinum* Δ*fadD28* + pCP0-*fadD28* (lanes 7a and 7b), *M. marinum* Δ*fadD29* + pCP0 (lanes 8a and 8b), and *M. marinum* Δ*fadD29* + pCP0-*fadD29* (lane 9a). The wild-type (wt) and mutant *M. marinum* strains carried the vector pCP0 so they could be cultured in the same kanamycin-containing medium used for the complemented strains. The TLC solvent systems used are as described for Fig. 4.

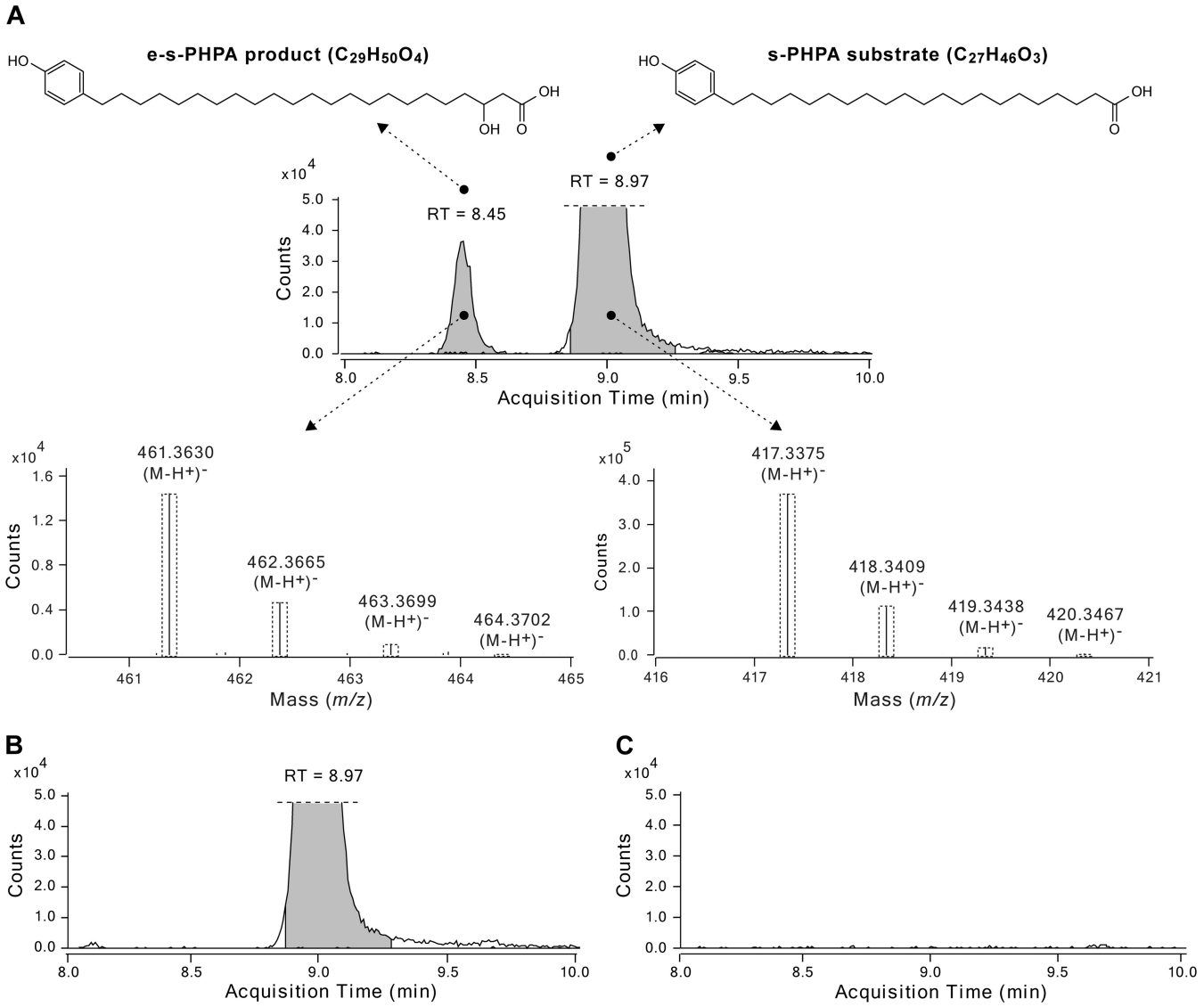

FIG 6 Extension of a synthetic PHPA substrate by the *M. marinum* FadD29-PpsA *in vitro* system. Extracted ion chromatogram and isotopic distributions for the synthetic PHPA substrate (s-PHPA) and the extended s-PHPA product (e-s-PHPA) in the complete reaction mixture (A) and extracted ion chromatograms from two representative negative-control reaction mixtures, i.e., one containing no malonyl-CoA (B) and the other no s-PHPA (C). The retention time (RT) is indicated in the chromatograms. The dashed-line boxes in the observed isotopic distributions indicate the calculated relative species abundance, which is in agreement with the experimental data.

Δ*fadD26*, *M. marinum* Δ*fadD28*, and *M. marinum* Δ*fadD29*), each with an unmarked, in-frame deletion in one of the four acyl-AMP ligase genes. We then examined the ability of the *M. marinum* mutants to produce PGLs and PDIMs by radio-TLC analysis.

The analysis of the PGL and PDIM production capacity of the *fadD* gene mutants revealed that deletion of *fadD28* led to a PGL$^-$ PDIM$^-$ phenotype (Fig. 5, cf. lanes 5a and 6a and cf. lanes 5b and 6b), deletion of *fadD26* produced selective loss of PDIMs (Fig. 5, cf. lanes 1a and 4a and cf. lanes 1b and 3b), and deletion of *fadD22* and *fadD29* led to selective loss of PGLs (Fig. 5, cf. lanes 1a and 2a and cf. lanes 1b and 2b for *fadD22* and cf. lanes 5a and 8a and cf. lanes 5b and 8b for *fadD29*). We also constructed and analyzed four corresponding genetic complementation control strains (*M. marinum* Δ*fadD22* + pCP0-*fadD22*, *M. marinum* Δ*fadD26* + pCP0-*fadD26*, *M. marinum* Δ*fadD28* + pCP0-*fadD28*, and *M. marinum* Δ*fadD29* + pCP0-*fadD29*). Each of these control strains carried a pCP0-based plasmid expressing the specific *fadD* gene deleted from the genome of the host strain. Radio-TLC analysis demonstrated that episomal expression of the *fadD* gene reasonably restored (fully or partially) the PGL and/or PDIM production capacity of each of the *M. marinum* mutants (Fig. 5, lanes 3a, 7a, 9a, 4b, and 7b). The complementation controls indicate that none of the deletions exerted a confounding polar effect preventing the functional assignment of the *fadD* genes. Overall, the findings of the mutational analysis of *fadD* genes conclusively demonstrate the specific roles of *fadD22*, *fadD26*, *fadD28*, and *fadD29* in PGL and/or PDIM production in *M. marinum* and, in conjunction with the available biochemical information establishing the function of the *p*-hydroxybenzoic acid-adenylating FadD22 protein (35, 36, 44), point at *M. marinum* FadD29 as the likely PHPA-

TABLE 1 LC-MS analysis of e-s-PHPA formation

Compound	Formula	Calculated $[(M\text{-}H^+)]^-$ *m/z*	Reaction mixture	Experimental $[(M\text{-}H^+)]^-$ *m/z*	Retention time (min)
s-PHPA	$C_{27}H_{46}O_3$	417.3374	Complete	417.3375	8.97
			No Mal-CoA	417.3374	8.97
			No NADPH	417.3373	9.01
			No ATP	417.3374	8.97
			No s-PHPA	ND[a]	
			No FadD29	417.3373	9.06
			No PpsA	417.3373	9.07
e-s-PHPA	$C_{29}H_{50}O_4$	461.3636	Complete	461.3630[b]	8.45
			No Mal-CoA	ND	
			No NADPH	ND	
			No ATP	ND	
			No s-PHPA	ND	
			No FadD29	ND	
			No PpsA	ND	

[a] ND, not detected.
[b] ppm = −1.37. Replicates rendered comparable experimental $[(M\text{-}H^+)]^-$ mass data, e.g., 461.3633 (ppm = −0.83), 461.3632 (ppm = −1.07).

specific AMP ligase involved in PHPA intermediate activation and loading onto PpsA in *M. marinum*. The conclusions supported by our mutational analysis in the nontuberculous mycobacterial species *M. marinum* parallel those derived from experiments in the *M. tuberculosis* complex (35, 44, 59).

An *in vitro*-reconstituted *M. marinum* FadD29-PpsA system displays PHPA intermediate activation, transfer, extension, and reduction capacity. Our mutational analysis in *M. marinum* supports the view that the Pks15/1-to-PpsA PHPA intermediate transfer takes place via the PHPA-AMP ligase-dependent pathway outlined in Fig. 3 (pathway A) and that FadD29 activates and loads PHPAs onto PpsA in *M. marinum*. We sought to further probe this mechanistic model by evaluating the ability of *M. marinum* FadD29 and *M. marinum* PpsA to functionally cooperate *in vitro* to produce an expected PHPA extended product. In these experiments, we utilized purified *M. marinum* FadD29 and PpsA proteins recombinantly produced in *E. coli*. Since PpsA was needed in its phosphopantetheinylated form, the synthase was coexpressed with the phosphopantetheinyl transferase Sfp to increase post-translational modification stoichiometry. Sfp is a robust enzyme from *Bacillus subtilis* (60) that we have previously used to phosphopantetheinylate recombinant *M. marinum* FadD22 and Pks15/1 proteins (35, 36).

We sought to use a predicted physiological PHPA substrate in these *in vitro* experiments. To this end, we used the synthetic PHPA substrate 21-(4-hydroxyphenyl)henicosanoic acid (s-PHPA; $C_{27}H_{46}O_3$), which was synthesized by a novel seven-step procedure (described in Fig. S4 in the supplemental material). The s-PHPA substrate corresponds to the released form of one of the most abundant PHPA intermediates produced by the *M. marinum* FadD22-Pks15/1 system *in vitro* and *in vivo* (36). By the canonical polyketide biosynthetic pathway predicted for PpsA based on its domain composition (13, 37) (Fig. 3), the s-PHPA substrate would be expected to be extended by two carbons via a KS domain-dependent decarboxylative Claisen condensation and to undergo ketoreductase (KR) domain-dependent β-keto group reduction to form the corresponding C29 acyl-PpsA thioester intermediate (Fig. 3). The competency of an *in vitro M. marinum* FadD29-PpsA system to catalyze the formation of this predicted s-PHPA-derived product was investigated by high-resolution LC-MS analysis of the extracted reaction product chemically released from the synthase by alkaline hydrolysis. Representative results of these studies are depicted in Fig. 6 and Table 1.

Gratifyingly, *in vitro* incubation of FadD29 and PpsA in the presence of s-PHPA substrate, malonyl-CoA (extender unit donor), ATP (for s-PHPA activation), and NADPH (for β-keto group reduction) led to the formation of a distinct s-PHPA-derived extended product (e-s-PHPA). The experimental mass for the e-s-PHPA product matched that calculated for 3-hydroxy-23-(4-hydroxyphenyl)tricosanoic acid ($C_{29}H_{50}O_4$; calculated *m/z* $[M\text{-}H^+]^-$ of 461.3636; experimental *m/z* $[M\text{-}H^+]^-$ of 461.3630), which is the expected released product after s-PHPA extension and reduction by PpsA (Fig. 6A; Table 1). Conversely, the e-s-PHPA product was not detected in control reaction mixtures lacking a single enzyme (FadD29 or PpsA) or a single substrate (malonyl-CoA, NADPH, ATP, or s-PHPA) (Table 1). The unreacted s-PHPA substrate was also detected in the complete reaction mixture ($C_{27}H_{46}O_3$; calculated *m/z* $[M\text{-}H^+]^-$ of 417.3374; experimental *m/z* $[M\text{-}H^+]^-$ of 417.3375) (Fig. 6A; Table 1). As expected, the s-PHPA substrate was detected by LC-MS in all control reaction mixtures lacking one of the enzymes or a substrate other than s-PHPA (e.g., malonyl-CoA [Fig. 6B]) but not in the control reaction mixture in which s-PHPA was omitted (Fig. 6C). Formation of the e-s-PHPA product was not observed in reaction mixtures in which FadD29 was replaced by recombinant *M. marinum* FadD26, although FadD26 was able to load a model fatty acid substrate (dodecanoic acid) on PpsA *in vitro* (not shown). The competency of *M. marinum* FadD26 to load PpsA with a fatty acyl starter unit is in line with the *in vitro* activity previously demonstrated for *M. tuberculosis* FadD26 (37, 52). The inability of *M. marinum* FadD26 to replace *M. marinum* FadD29 *in vitro* is consistent with our finding that *M. marinum* Δ*fadD29* is PGL deficient despite having *fadD26* (Fig. 5A). Altogether, the results with the reconstituted *M. marinum* FadD29-PpsA system demonstrate that *M. marinum* FadD29 and *M. marinum* PpsA cooperate *in vitro* to produce an expected PHPA extended product and support the genetic studies identifying FadD29 as the PHPA-AMP ligase required for PGL biosynthesis in *M. marinum*. Overall, the *M.*

marinum FadD29-PpsA *in vitro* system appears to be competent to catalyze PHPA activation, loading, extension, and reduction in line with the model proposed in Fig. 3. The *M. marinum* FadD29-PpsA *in vitro* system along with the *M. marinum* FadD22-Pks15/1 *in vitro* system for biosynthesis of PHPAs that we have developed previously (36) lays a valuable foundation for further mechanistic analysis of the enzymatic machinery involved in PGL biosynthesis in *M. marinum*.

The *M. marinum* FadD29-PpsA functional partnership established by our *in vitro* studies represents the first acyl-AMP ligase and type I PKS partnership for acyl starter unit activation and PKS loading established in nontuberculous mycobacteria. Three analogous partnerships have been demonstrated in *M. tuberculosis*. These are the FadD26-PpsA partnership noted above for PDIM production (37, 52), a FadD32-Pks13 partnership that takes place during mycolic acid biosynthesis (52, 61, 62), and a FadD30-Pks6 partnership believed to be required for production of novel polar lipids (52, 63). To our knowledge, however, the partially overlapping PGL/PDIM biosynthetic pathways provide the first example of two distinct acyl-AMP ligases (i.e., FadD29 and FadD26) loading the same type I PKS (i.e., PpsA) with two alternate starter units (i.e., PHPAs and fatty acids). This bimodal loading strategy allows the bacterium to use the PpsABCDE megasynthase system to generate two structurally different products. Interestingly, recent host-pathogen interaction studies suggest that *M. marinum* PGLs and *M. marinum* PDIMs have different roles within a complex immune evasion mechanism (15). It will be interesting to investigate whether the FadD29-PpsA versus FadD26-PpsA alternative partnership is utilized by the pathogen as a control point to modulate the relative abundance of PGLs and PDIMs in the cell.

ACKNOWLEDGMENTS

This work was supported in part by NIH grant R15AI105884 awarded to L.E.N.Q. We are grateful for the endowment support from Carol and Larry Zicklin and acknowledge the support from instrumentation grant NSF-CHE-MRI 1228921.

We thank Yasmin Chen (L.E.N.Q. laboratory) for assistance with mutant constructions. We are grateful to Chaitan Khosla (Stanford University) for providing *E. coli* BAP1.

REFERENCES

1. **Dye C, Williams BG.** 2010. The population dynamics and control of tuberculosis. Science **328:**856–861. http://dx.doi.org/10.1126/science.1185449.
2. **Gopinath K, Singh S.** 2010. Non-tuberculous mycobacteria in TB-endemic countries: are we neglecting the danger? PLoS Negl Trop Dis **4:**e615. http://dx.doi.org/10.1371/journal.pntd.0000615.
3. **Scollard DM, Adams LB, Gillis TP, Krahenbuhl JL, Truman RW, Williams DL.** 2006. The continuing challenges of leprosy. Clin Microbiol Rev **19:**338–381. http://dx.doi.org/10.1128/CMR.19.2.338-381.2006.
4. **WHO.** 2014. Global tuberculosis report. World Health Organization, Geneva, Switzerland.
5. **Rodrigues LC, Lockwood D.** 2011. Leprosy now: epidemiology, progress, challenges, and research gaps. Lancet Infect Dis **11:**464–470. http://dx.doi.org/10.1016/S1473-3099(11)70006-8.
6. **Brennan PJ, Nikaido H.** 1995. The envelope of mycobacteria. Annu Rev Biochem **64:**29–63. http://dx.doi.org/10.1146/annurev.bi.64.070195.000333.
7. **Crick DC, Quadri LE, Brennan PJ.** 2008. Biochemistry of the cell envelope of *Mycobacterium tuberculosis*, p 1–20. *In* Kaufmann SHE, Rubin R (ed), Handbook of tuberculosis: molecular biology and biochemistry. Wiley-VCH Verlag GmbH & Co. KgaA, Weinheim, Germany.
8. **Minnikin DE, Kremer L, Dover LG, Besra GS.** 2002. The methyl-branched fortifications of *Mycobacterium tuberculosis*. Chem Biol **9:**545–553. http://dx.doi.org/10.1016/S1074-5521(02)00142-4.
9. **Niederweis M, Danilchanka O, Huff J, Hoffmann C, Engelhardt H.** 2010. Mycobacterial outer membranes: in search of proteins. Trends Microbiol **18:**109–116. http://dx.doi.org/10.1016/j.tim.2009.12.005.
10. **Daffé M.** 2008. The global architecture of the mycobacterial cell envelope, p 3–11. *In* Daffe M, Reyrat JM (ed), The mycobacterial cell envelope. ASM Press, Washington, DC.
11. **Angala SK, Belardinelli JM, Huc-Claustre E, Wheat WH, Jackson M.** 2014. The cell envelope glycoconjugates of *Mycobacterium tuberculosis*. Crit Rev Biochem Mol Biol **49:**361–399. http://dx.doi.org/10.3109/10409238.2014.925420.
12. **Neyrolles O, Guilhot C.** 2011. Recent advances in deciphering the contribution of *Mycobacterium tuberculosis* lipids to pathogenesis. Tuberculosis (Edinb) **91:**187–195. http://dx.doi.org/10.1016/j.tube.2011.01.002.
13. **Onwueme KC, Vos CJ, Zurita J, Ferreras JA, Quadri LE.** 2005. The dimycocerosate ester polyketide virulence factors of mycobacteria. Prog Lipid Res **44:**259–302. http://dx.doi.org/10.1016/j.plipres.2005.07.001.
14. **Astarie-Dequeker C, Le Guyader L, Malaga W, Seaphanh FK, Chalut C, Lopez A, Guilhot C.** 2009. Phthiocerol dimycocerosates of *M. tuberculosis* participate in macrophage invasion by inducing changes in the organization of plasma membrane lipids. PLoS Pathog **5:**e1000289. http://dx.doi.org/10.1371/journal.ppat.1000289.
15. **Cambier CJ, Takaki KK, Larson RP, Hernandez RE, Tobin DM, Urdahl KB, Cosma CL, Ramakrishnan L.** 2014. Mycobacteria manipulate macrophage recruitment through coordinated use of membrane lipids. Nature **505:**218–222. http://dx.doi.org/10.1038/nature12799.
16. **Cox JS, Chen B, McNeil M, Jacobs WR, Jr.** 1999. Complex lipid determines tissue-specific replication of *Mycobacterium tuberculosis* in mice. Nature **402:**79–83. http://dx.doi.org/10.1038/47042.
17. **Passemar C, Arbues A, Malaga W, Mercier I, Moreau F, Lepourry L, Neyrolles O, Guilhot C, Astarie-Dequeker C.** 2014. Multiple deletions in the polyketide synthase gene repertoire of *Mycobacterium tuberculosis* reveal functional overlap of cell envelope lipids in host-pathogen interactions. Cell Microbiol **16:**195–213. http://dx.doi.org/10.1111/cmi.12214.
18. **Reed MB, Domenech P, Manca C, Su H, Barczak AK, Kreiswirth BN, Kaplan G, Barry CE, III.** 2004. A glycolipid of hypervirulent tuberculosis strains that inhibits the innate immune response. Nature **431:**84–87. http://dx.doi.org/10.1038/nature02837.
19. **Tsenova L, Ellison E, Harbacheuski R, Moreira AL, Kurepina N, Reed MB, Mathema B, Barry CE, III, Kaplan G.** 2005. Virulence of selected *Mycobacterium tuberculosis* clinical isolates in the rabbit model of meningitis is dependent on phenolic glycolipid produced by the bacilli. J Infect Dis **192:**98–106. http://dx.doi.org/10.1086/430614.
20. **Yu J, Tran V, Li M, Huang X, Niu C, Wang D, Zhu J, Wang J, Gao Q, Liu J.** 2012. Both phthiocerol dimycocerosates and phenolic glycolipids are required for virulence of *Mycobacterium marinum*. Infect Immun **80:**1381–1389. http://dx.doi.org/10.1128/IAI.06370-11.
21. **Tabouret G, Astarie-Dequeker C, Demangel C, Malaga W, Constant P, Ray A, Honore N, Bello NF, Perez E, Daffe M, Guilhot C.** 2010. *Mycobacterium leprae* phenolglycolipid-1 expressed by engineered *M. bovis* BCG modulates early interaction with human phagocytes. PLoS Pathog **6:**e1001159. http://dx.doi.org/10.1371/journal.ppat.1001159.
22. **Alibaud L, Rombouts Y, Trivelli X, Burguiere A, Cirillo SL, Cirillo JD, Dubremetz JF, Guerardel Y, Lutfalla G, Kremer L.** 2011. A *Mycobacterium marinum* TesA mutant defective for major cell wall-associated lipids is highly attenuated in *Dictyostelium discoideum* and zebrafish embryos. Mol Microbiol **80:**919–934. http://dx.doi.org/10.1111/j.1365-2958.2011.07618.x.
23. **Brodin P, Poquet Y, Levillain F, Peguillet I, Larrouy-Maumus G, Gilleron M, Ewann F, Christophe T, Fenistein D, Jang J, Jang MS, Park SJ, Rauzier J, Carralot JP, Shrimpton R, Genovesio A, Gonzalo-Asensio JA, Puzo G, Martin C, Brosch R, Stewart GR, Gicquel B, Neyrolles O.** 2010. High content phenotypic cell-based visual screen identifies *Mycobacterium tuberculosis* acyltrehalose-containing glycolipids involved in phagosome remodeling. PLoS Pathog **6:**e1001100. http://dx.doi.org/10.1371/journal.ppat.1001100.
24. **Collins DM, Skou B, White S, Bassett S, Collins L, For R, Hurr K, Hotter G, de Lisle GW.** 2005. Generation of attenuated *Mycobacterium bovis* strains by signature-tagged mutagenesis for discovery of novel vaccine candidates. Infect Immun **73:**2379–2386. http://dx.doi.org/10.1128/IAI.73.4.2379-2386.2005.
25. **Camacho LR, Ensergueix D, Perez E, Gicquel B, Guilhot C.** 1999. Identification of a virulence gene cluster of *Mycobacterium tuberculosis* by signature-tagged transposon mutagenesis. Mol Microbiol **34:**257–267. http://dx.doi.org/10.1046/j.1365-2958.1999.01593.x.

26. **Murry JP, Pandey AK, Sassetti CM, Rubin EJ.** 2009. Phthiocerol dimycocerosate transport is required for resisting interferon-gamma-independent immunity. J Infect Dis **200:**774–782. http://dx.doi.org/10.1086/605128.
27. **Ng V, Zanazzi G, Timpl R, Talts JF, Salzer JL, Brennan PJ, Rambukkana A.** 2000. Role of the cell wall phenolic glycolipid-1 in the peripheral nerve predilection of *Mycobacterium leprae*. Cell **103:**511–524. http://dx.doi.org/10.1016/S0092-8674(00)00142-2.
28. **Rambukkana A, Zanazzi G, Tapinos N, Salzer JL.** 2002. Contact-dependent demyelination by *Mycobacterium leprae* in the absence of immune cells. Science **296:**927–931. http://dx.doi.org/10.1126/science.1067631.
29. **Ruley KM, Ansede JH, Pritchett CL, Talaat AM, Reimschuessel R, Trucksis M.** 2004. Identification of *Mycobacterium marinum* virulence genes using signature-tagged mutagenesis and the goldfish model of mycobacterial pathogenesis. FEMS Microbiol Lett **232:**75–81. http://dx.doi.org/10.1016/S0378-1097(04)00017-5.
30. **Robinson N, Kolter T, Wolke M, Rybniker J, Hartmann P, Plum G.** 2008. Mycobacterial phenolic glycolipid inhibits phagosome maturation and subverts the pro-inflammatory cytokine response. Traffic **9:**1936–1947. http://dx.doi.org/10.1111/j.1600-0854.2008.00804.x.
31. **Sinsimer D, Huet G, Manca C, Tsenova L, Koo MS, Kurepina N, Kana B, Mathema B, Marras SA, Kreiswirth BN, Guilhot C, Kaplan G.** 2008. The phenolic glycolipid of *Mycobacterium tuberculosis* differentially modulates the early host cytokine response but does not in itself confer hypervirulence. Infect Immun **76:**3027–3036. http://dx.doi.org/10.1128/IAI.01663-07.
32. **Rousseau C, Winter N, Pivert E, Bordat Y, Neyrolles O, Ave P, Huerre M, Gicquel B, Jackson M.** 2004. Production of phthiocerol dimycocerosates protects *Mycobacterium tuberculosis* from the cidal activity of reactive nitrogen intermediates produced by macrophages and modulates the early immune response to infection. Cell Microbiol **6:**277–287. http://dx.doi.org/10.1046/j.1462-5822.2004.00368.x.
33. **Camacho LR, Constant P, Raynaud C, Laneelle MA, Triccas JA, Gicquel B, Daffe M, Guilhot C.** 2001. Analysis of the phthiocerol dimycocerosate locus of *Mycobacterium tuberculosis*. Evidence that this lipid is involved in the cell wall permeability barrier. J Biol Chem **276:**19845–19854. http://dx.doi.org/10.1074/jbc.M100662200.
34. **Chavadi SS, Edupuganti UR, Vergnolle O, Fatima I, Singh SM, Soll CE, Quadri LE.** 2011. Inactivation of *tesA* reduces cell wall lipid production and increases drug susceptibility in mycobacteria. J Biol Chem **286:**24616–24625. http://dx.doi.org/10.1074/jbc.M111.247601.
35. **Ferreras JA, Stirrett KL, Lu X, Ryu JS, Soll CE, Tan DS, Quadri LE.** 2008. Mycobacterial phenolic glycolipid virulence factor biosynthesis: mechanism and small-molecule inhibition of polyketide chain initiation. Chem Biol **15:**51–61. http://dx.doi.org/10.1016/j.chembiol.2007.11.010.
36. **He W, Soll CE, Chavadi SS, Zhang G, Warren JD, Quadri LE.** 2009. Cooperation between a coenzyme A-independent stand-alone initiation module and an iterative type I polyketide synthase during synthesis of mycobacterial phenolic glycolipids. J Am Chem Soc **131:**16744–16750. http://dx.doi.org/10.1021/ja904792q.
37. **Trivedi OA, Arora P, Vats A, Ansari MZ, Tickoo R, Sridharan V, Mohanty D, Gokhale RS.** 2005. Dissecting the mechanism and assembly of a complex virulence mycobacterial lipid. Mol Cell **17:**631–643. http://dx.doi.org/10.1016/j.molcel.2005.02.009.
38. **Azad AK, Sirakova TD, Fernandes ND, Kolattukudy PE.** 1997. Gene knockout reveals a novel gene cluster for the synthesis of a class of cell wall lipids unique to pathogenic mycobacteria. J Biol Chem **272:**16741–16745. http://dx.doi.org/10.1074/jbc.272.27.16741.
39. **Tobin DM, Ramakrishnan L.** 2008. Comparative pathogenesis of *Mycobacterium marinum* and *Mycobacterium tuberculosis*. Cell Microbiol **10:**1027–1039. http://dx.doi.org/10.1111/j.1462-5822.2008.01133.x.
40. **Cosma CL, Humbert O, Ramakrishnan L.** 2004. Superinfecting mycobacteria home to established tuberculous granulomas. Nat Immunol **5:**828–835. http://dx.doi.org/10.1038/ni1091.
41. **Stamm LM, Brown EJ.** 2004. *Mycobacterium marinum*: the generalization and specialization of a pathogenic mycobacterium. Microbes Infect **6:**1418–1428. http://dx.doi.org/10.1016/j.micinf.2004.10.003.
42. **Stinear TP, Seemann T, Harrison PF, Jenkin GA, Davies JK, Johnson PD, Abdellah Z, Arrowsmith C, Chillingworth T, Churcher C, Clarke K, Cronin A, Davis P, Goodhead I, Holroyd N, Jagels K, Lord A, Moule S, Mungall K, Norbertczak H, Quail MA, Rabbinowitsch E, Walker D, White B, Whitehead S, Small PL, Brosch R, Ramakrishnan L, Fischbach MA, Parkhill J, Cole ST.** 2008. Insights from the complete genome sequence of *Mycobacterium marinum* on the evolution of *Mycobacterium tuberculosis*. Genome Res **18:**729–741. http://dx.doi.org/10.1101/gr.075069.107.
43. **Quadri LE.** 2014. Biosynthesis of mycobacterial lipids by polyketide synthases and beyond. Crit Rev Biochem Mol Biol **49:**179–211. http://dx.doi.org/10.3109/10409238.2014.896859.
44. **Simeone R, Leger M, Constant P, Malaga W, Marrakchi H, Daffe M, Guilhot C, Chalut C.** 2010. Delineation of the roles of FadD22, FadD26 and FadD29 in the biosynthesis of phthiocerol dimycocerosates and related compounds in *Mycobacterium tuberculosis*. FEBS J **277:**2715–2725. http://dx.doi.org/10.1111/j.1742-4658.2010.07688.x.
45. **Parish T, Stoker NG.** 1998. Mycobacteria protocols. *In* Walker JM (ed), Methods in molecular biology, vol 101. Humana Press, Totowa, NJ.
46. **Sambrook J, Russell DW.** 2001. Molecular cloning: a laboratory manual, 3rd ed. Cold Spring Harbor Press, Cold Spring Harbor, NY.
47. **Parish T, Stoker NG.** 2000. Use of a flexible cassette method to generate a double unmarked *Mycobacterium tuberculosis tlyA plcABC* mutant by gene replacement. Microbiology **146:**1969–1975.
48. **Onwueme KC, Ferreras JA, Buglino J, Lima CD, Quadri LE.** 2004. Mycobacterial polyketide-associated proteins are acyltransferases: proof of principle with *Mycobacterium tuberculosis* PapA5. Proc Natl Acad Sci U S A **101:**4608–4613. http://dx.doi.org/10.1073/pnas.0306928101.
49. **Horton RM, Hunt HD, Ho SN, Pullen JK, Pease LR.** 1989. Engineering hybrid genes without the use of restriction enzymes: gene splicing by overlap extension. Gene **77:**61–68. http://dx.doi.org/10.1016/0378-1119(89)90359-4.
50. **Chavadi S, Onwueme K, Edupuganti U, Jerome J, Chatterjee D, Soll C, Quadri L.** 2012. The mycobacterial acyltransferase PapA5 is required for biosynthesis of cell wall-associated phenolic glycolipids. Microbiology **158:**1379–1387. http://dx.doi.org/10.1099/mic.0.057869-0.
51. **Pfeifer BA, Admiraal SJ, Gramajo H, Cane DE, Khosla C.** 2001. Biosynthesis of complex polyketides in a metabolically engineered strain of *E. coli*. Science **291:**1790–1792. http://dx.doi.org/10.1126/science.1058092.
52. **Trivedi OA, Arora P, Sridharan V, Tickoo R, Mohanty D, Gokhale RS.** 2004. Enzymic activation and transfer of fatty acids as acyl-adenylates in mycobacteria. Nature **428:**441–445. http://dx.doi.org/10.1038/nature02384.
53. **Beck BJ, Yoon YJ, Reynolds KA, Sherman DH.** 2002. The hidden steps of domain skipping: macrolactone ring size determination in the pikromycin modular polyketide synthase. Chem Biol **9:**575–583. http://dx.doi.org/10.1016/S1074-5521(02)00146-1.
54. **Tang GL, Cheng YQ, Shen B.** 2006. Polyketide chain skipping mechanism in the biosynthesis of the hybrid nonribosomal peptide-polyketide antitumor antibiotic leinamycin in Streptomyces atroolivaceus S-140. J Nat Prod **69:**387–393. http://dx.doi.org/10.1021/np050467t.
55. **Tang L, Ward S, Chung L, Carney JR, Li Y, Reid R, Katz L.** 2004. Elucidating the mechanism of cis double bond formation in epothilone biosynthesis. J Am Chem Soc **126:**46–47. http://dx.doi.org/10.1021/ja030503f.
56. **Fischbach MA, Walsh CT.** 2006. Assembly-line enzymology for polyketide and nonribosomal peptide antibiotics: logic, machinery, and mechanisms. Chem Rev **106:**3468–3496. http://dx.doi.org/10.1021/cr0503097.
57. **Walsh CT, Gehring AM, Weinreb PH, Quadri LE, Flugel RS.** 1997. Post-translational modification of polyketide and nonribosomal peptide synthases. Curr Opin Chem Biol **1:**309–315. http://dx.doi.org/10.1016/S1367-5931(97)80067-1.
58. **Lai JR, Koglin A, Walsh CT.** 2006. Carrier protein structure and recognition in polyketide and nonribosomal peptide biosynthesis. Biochemistry **45:**14869–14879. http://dx.doi.org/10.1021/bi061979p.
59. **Fitzmaurice AM, Kolattukudy PE.** 1998. An acyl-CoA synthase (*acoas*) gene adjacent to the mycocerosic acid synthase (*mas*) locus is necessary for mycocerosyl lipid synthesis in *Mycobacterium tuberculosis var*. bovis BCG. J Biol Chem **273:**8033–8039. http://dx.doi.org/10.1074/jbc.273.14.8033.
60. **Quadri LEN, Weinreb PH, Lei M, Nakano MM, Zuber P, Walsh CT.** 1998. Characterization of Sfp, a *Bacillus subtilis* phosphopantetheinyl transferase for peptidyl carrier protein domains in peptide synthetases. Biochemistry **37:**1585–1595. http://dx.doi.org/10.1021/bi9719861.
61. **Gavalda S, Leger M, van der Rest B, Stella A, Bardou F, Montrozier H, Chalut C, Burlet-Schiltz O, Marrakchi H, Daffé M, Quemard A.** 2009. The Pks13/FadD32 crosstalk for the biosynthesis of mycolic acids in *Mycobacterium tuberculosis*. J Biol Chem **284:**19255–19264. http://dx.doi.org/10.1074/jbc.M109.006940.

62. **Leger M, Gavalda S, Guillet V, van der Rest B, Slama N, Montrozier H, Mourey L, Quemard A, Daffé M, Marrakchi H.** 2009. The dual function of the *Mycobacterium tuberculosis* FadD32 required for mycolic acid biosynthesis. Chem Biol **16:**510–519. http://dx.doi.org/10.1016/j.chembiol.2009.03.012.
63. **Waddell SJ, Chung GA, Gibson KJ, Everett MJ, Minnikin DE, Besra GS, Butcher PD.** 2005. Inactivation of polyketide synthase and related genes results in the loss of complex lipids in *Mycobacterium tuberculosis* H37Rv. Lett Appl Microbiol **40:**201–206. http://dx.doi.org/10.1111/j.1472-765X.2005.01659.x.
64. **Constant P, Perez E, Malaga W, Laneelle MA, Saurel O, Daffe M, Guilhot C.** 2002. Role of the *pks15/1* gene in the biosynthesis of phenolglycolipids in the *M. tuberculosis* complex: evidence that all strains synthesize glycosylated *p*-hydroxybenzoic methyl esters and that strains devoid of phenolglycolipids harbor a frameshift mutation in the *pks15/1* gene. J Biol Chem **277:**38148–38158. http://dx.doi.org/10.1074/jbc.M206538200.